

Silicon Solar Cells Parameters Optimization by Adequate Surface Processing Techniques

E. MANEA¹, E. BUDIANU¹, M. PURICA¹, C. PODARU¹,
A. POPESCU¹, C. PARVULESCU¹, A. DINESCU¹,
A. CORACI¹, I.CERNICA¹, F. BABARADA²

¹National Institute for Research and Development in Microtechnologies,
72996 Bucharest, Romania

E-mail: elenam@imt.ro

² Faculty of Electronic and Telecommunication,
Politehnica University of Bucharest, Romania

Abstract. This paper presents the results of an experimental study regarding the increase in the efficiency of the silicon solar cells, using various methods for texturing the front surface. Designing, patterning and surface etching processes led to obtain reined structures with very low losses of the incident optical radiation. This paper aims to compare the fabrication method using the proposed textured surfaces with the standard method.

Key words: texturization, silicon, porous silicon, anodic oxidation films, solar cells.

1. Introduction

The solar cells and the technological processes necessary for their realization are often used as research, design and fabrication objectives because of their importance in electrical energy generation. Are used, especially, those materials and technologies which lead to a greater efficiency and lower costs. The basic material in solar cell fabrication is monocrystalline silicon because of the great efficiency (maximum 24.7%), of its advanced technologies of manufacturing and its reliability (over 25 year's exploitation) [1–4]. However, there are still methods able to increase the efficiency

in industrial fabrication, to simplify the technological processes (still expensive) and to obtain a cheaper and higher quality material. Also, in exploitation of the solar cells, there are other problems concerning the space orientation, reflection elimination on the cell surface, the dissipation of heat resulted from the radiations that do not participate to the photovoltaic conversion etc. Some of these problems concern the photovoltaic cell, and some of them deal with the organization of the solar modulus. In order to obtain a maximum yield and good reliability we must take into account the pair modulus – cells. There is always a concern to change the technologies and materials of fabrication of the solar cells.

In solar cell fabrication a way of increasing efficiency consists in the elimination of the solar radiation losses on the surface.

2. Experimental

For the structuring processes of the high efficiency solar cell surface it was used p-type, $< 100 >$ monocrystalline silicon wafers (doped with boron) having 3" diameter, thickness 380 μm , and 1–2 Ωcm resistivity.

There were studied three types of surface structures: honeycomb structure, regular pyramids structure and electrochemical porosification of the silica. The first two structural types were obtained using technological processes from planar technology of the integrated circuit consisting in:

- the rising on the surface of the silicon wafer of a silicon dioxide layer of 800 nm thickness used as etching mask;
- a photolithographic process based on positive photoresist, where patterned windows in silicon dioxide have been realized.

In the case of honeycomb type, the windows are 4 μm , respectively 6 μm in diameter and they are uniformly spaced in the vertex of an equilateral triangle with 20 μm side on whole surface of silicon wafer. Through the window opened in the oxide, silicon has been isotropically etched in two types of acid solution HNO_3 : HF : NH_4F : H_2O – (280:3:6:140) and HNO_3 : HF : CH_3COOH – (25:1:10) [5]. In order to form semi – spherical walls. The moment when these walls touch the neighbor semi-spherical walls, hexagonal structures are formed; this being put in evidence by the SEM images of the texturing surface taken through oxide, as shown in Fig. 1.

The etching depth is 7 μm and 5 μm , respectively.

For the case of pyramidal texturisation of silicon wafers, in silicon dioxide were patterned square windows with the side of 20 μm and 10 μm , respectively. For silicon etching in these windows we have used a 40% KOH solution at 80°C temperature.

Porous silicon is a material that has been applied in solar cells, essentially as antireflection coating, due to low reflectance values.

Porous silicon samples used in photovoltaic applications were prepared by electrochemical etching on p-silicon wafers $< 100 >$, phosphorous doped and HF : $\text{C}_2\text{H}_5\text{OH}$: H_2O – (2:2:1) as electrolyte. The current density range, 5 to 18 mA/cm^2 , anodisation time, 600 s, illumination, a 500 W halogen lamp, $T = 23^\circ\text{C}$.

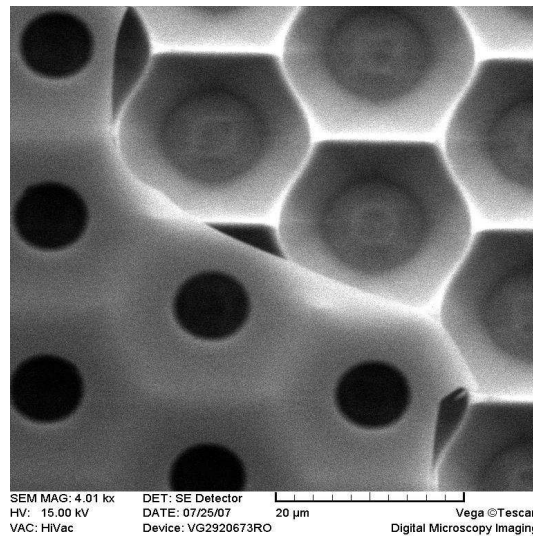


Fig. 1. SEM image of the structure through oxide.

3. Results and discussion

Texturized surfaces obtained have been analyzed by scanning electron microscopy (SEM) and spectrophotometric measurements.

In the case of honeycomb texturization two types of acid solutions have been used, HNO_3 : HF: CH_3COOH – (25:1:10) and HNO_3 : HF: NH_4F : H_2O – (280:3:6:140) for the silicon isotropic etch by oxide mask having 6 µm and 4 µm.

For the solution HNO_3 : HF: NH_4F : H_2O – (280:3:6:140), etch time is 10 times shorter compared to the solution HNO_3 : HF: CH_3COOH – (25:1:10), this leading to texturized surfaces uniform on the whole silicon wafer area and to a good control of the etch time (the neighboring walls become in contact).

Figure 2 presents a SEM image of an intermediate etch putting in evidence the hemispherical shape of the walls and the bottom shape of the structure etched in acid solution.

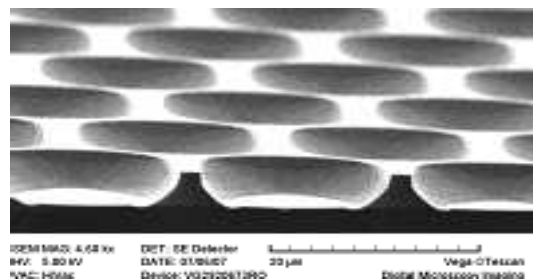


Fig. 2. SEM image of an intermediate etch etched in acid solution HNO_3 : HF: CH_3COOH – (25:1:10) by the 6 µm window.

Figure 3 presents a perspective view of SEM image of the surface etched in acid solution HNO_3 : HF : NH_4F : H_2O – (280:3:6:140) through a window of 6 μm . The hexagon diagonal is 20 μm and the etch depth is 5 μm for structures etched by the 6 μm window.

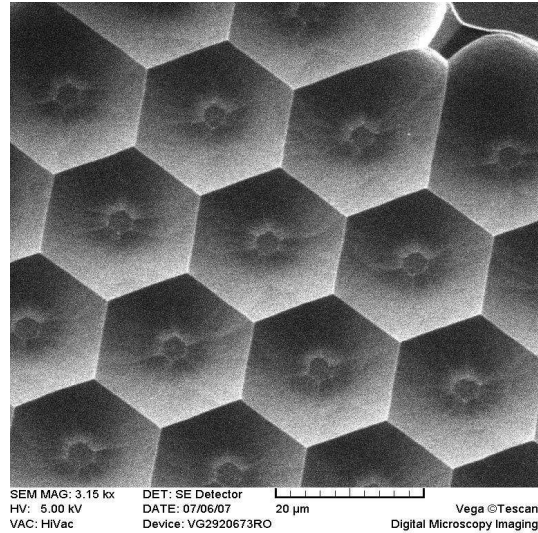


Fig. 3. SEM image of the surface etched in acid solution HNO_3 : HF : NH_4F : H_2O – (280:3:6:140) through a window of 4 μm ; perspective view of the surface.

Figure 4 presents the detailed SEM image for honeycomb structures etched in acid solution HNO_3 : HF : CH_3COOH – (25:1:10) by the 6 μm window.

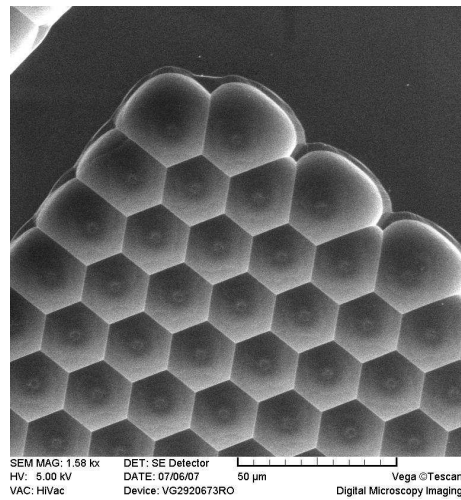


Fig. 4. SEM image for honeycomb structures etched in acid solution HNO_3 : HF : CH_3COOH – (25:1:10) by the 6 μm window; detailed of the surface.

By comparison, from the images presented in Fig. 3 and Fig. 4 it can be observed the similarities realized etching using the two aforementioned acid solutions etching. However, some differences were put in evidence for the two type of acid solutions by spectrophotometry.

Onto the same silicon substrate was studied also the surface texturization in pyramids up-side-downed having the period from 20 μm to 10 μm , obtained by photolithography. The silicon was anisotropically etched in solution 40% KOH at 80°C by oxide mask.

Figure 5 presents the SEM image of a section in the pyramidal textured structure.

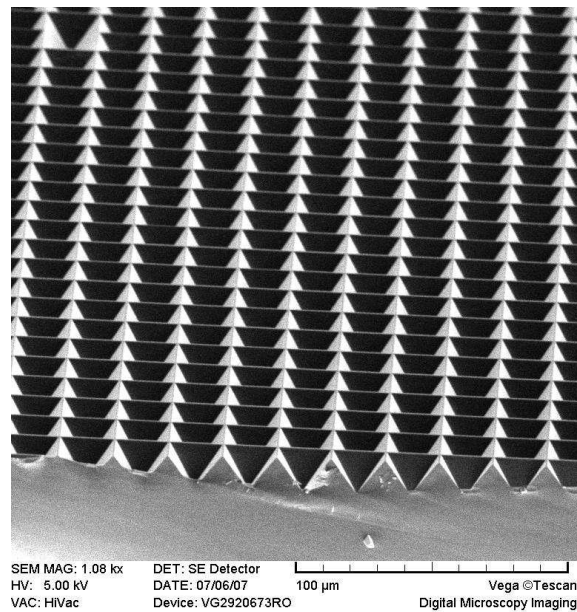


Fig. 5. SEM image of a section in the pyramidal textured structure.

4. Characterization

The obtained texturing surfaces were characterized by spectrophotometric measurements.

The reflectance spectra of the textured (using different solutions and patterning geometries) silicon wafers and the porous silicon layer have been studied in the wavelength range from 350 nm to 900 nm using a SPECORD – M42 double beam spectrophotometer.

Spectral reflectance measurements obtained for textured (using different solutions and patterning geometries) silicon wafers are presented in Fig. 6 and Fig. 7.

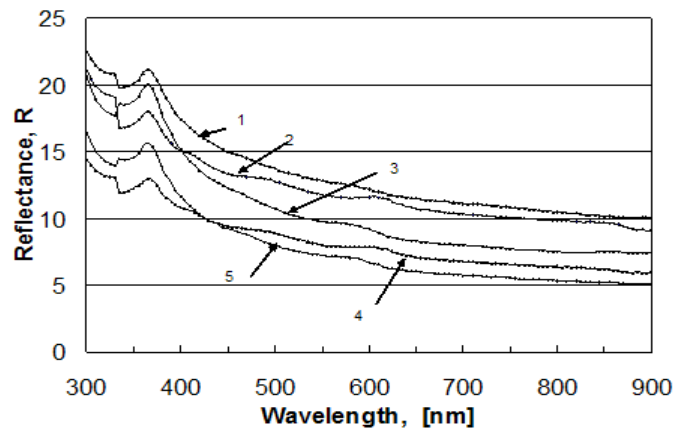


Fig. 6. Spectral Reflectance of the textured silicon $\langle 100 \rangle$ surface without anti reflection film.

In Fig. 6 are presented spectra for textured probes without anti reflection film and for a silicon wafer mechano-chemical polished, usually used in the monocrystallin silicon solar cells technology. Their analysis shows that texturization leads to an reflectance decrement (under 30%) indifferently of the geometry and etch solution. In the interest field for solar cells the reflectance has values in the domain of 5–12%. These curves reveal the increasing importance of the geometry comparing to the etch solution. Therefore, in the case of $\langle 100 \rangle$ silicon anisotropic etching for the pyramidal geometry in the same solution (40% KOH at 80°C) it was observed a smaller reflectance corresponding to a geometry having smaller side ($w = 20 \mu\text{m}$) see curve 3, compared with the case $w = 10 \mu\text{m}$, curve 5 in Fig. 6. The same geometry dependence was observed in the honeycomb using the solution $\text{HNO}_3 : \text{HF} : \text{NH}_4\text{F} : \text{H}_2\text{O} - (280:3:6:140)$, see curve 1 and 4 corresponding to the initial windows diameters of $6 \mu\text{m}$ and $4 \mu\text{m}$, respectively. The difference in reflectance is smaller for the curve 1 and 2 for textured samples using the the same geometry but different etch solutions, $\text{HNO}_3 : \text{HF} : \text{NH}_4\text{F} : \text{H}_2\text{O} - (280:3:6:140)$ and $\text{HNO}_3 : \text{HF} : \text{CH}_3\text{COOH} - (25:1:10)$, respectively. This shows that it is more efficient to use the solution $\text{HNO}_3 : \text{HF} : \text{NH}_4\text{F} : \text{H}_2\text{O} - (280:3:6:140)$ which has a lower etch rate.

To maintain the reflectance under 10%, are used texturization geometries having small openings, see curve 4 and 5 in both cases of anisotropic etch in 40% KOH al 80°C, and also for the isotropic $\text{HNO}_3 : \text{HF} : \text{NH}_4\text{F} : \text{H}_2\text{O} - (280:3:6:140)$ and $\text{HNO}_3 : \text{HF} : \text{CH}_3\text{COOH} - (25:1:10)$.

Figure 7 presents reflectances for the textured samples in the same conditions as the previous ones, but having an anti reflectant SiO_2 layer, with thickness 154 nm for $\lambda = 0.900 \mu\text{m}$.

Reflectance values are smaller than in the previous case decreasing under 5% for $\lambda > 0.750 \text{ nm}$. For comparison are presented curves for an untextured surface covered with an anti reflectant layer and curve 2 corresponding to a intermediate honeycomb texturization.

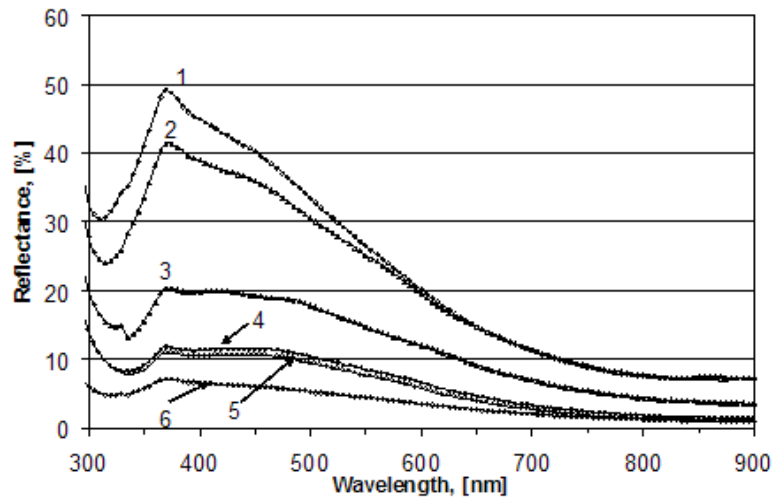


Fig. 7. Spectral Reflectance of the texturized silicon $\langle 100 \rangle$ surface with anti reflection film: Curve 1- untextured surface; Curves 2, 3, 6 – honeycomb type texturized surface by isotropic etching (curve 2 – $w = 6 \mu\text{m}$ in $\text{HNO}_3:\text{HF}:\text{CH}_3\text{COOH}$ (25:1:10); curve 3 – $w = 4 \mu\text{m}$ in $\text{HNO}_3:\text{H}_2\text{O}:\text{NH}_4\text{F}:\text{HF}$ -(280:140: 6: 3); curve 6 – $w = 6 \mu\text{m}$ in $\text{HNO}_3:\text{H}_2\text{O}:\text{NH}_4\text{F}:\text{HF}$ -(280:140: 6: 3); Curves 4, 5 – pyramid type texturized surface in KOH 40% at 80°C (curve 4 – $w = 10 \mu\text{m}$; curve 5 – $w = 20 \mu\text{m}$).

The reflectance values for n^+ porous silicon, obtained by anodic oxidation of the crystalline silicon wafers in a mixture of hydrofluoric acid and ethanol at current density range 5 to $18 \text{ mA}/\text{cm}^2$, and for initial Si wafer are shown in Fig. 8.

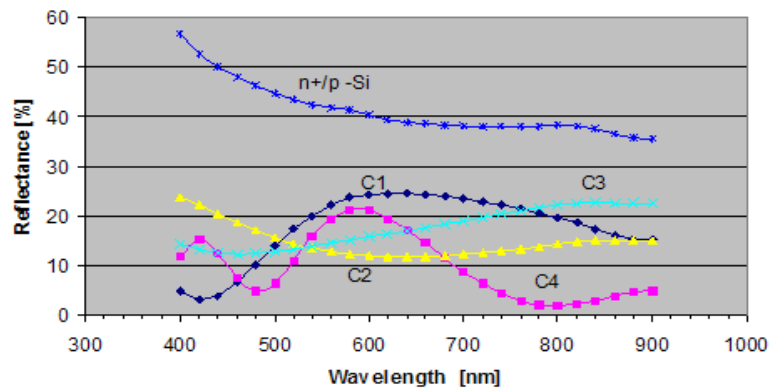


Fig. 8. Spectral dependence of reflectance for porous silicon samples and reference.

It can be seen that the reflectance of the porous layers is lower than reference sample ($n^+/\text{p Si}$).

Gravimetric measurements were used to determine the average density of the analyzed porous layers. Thickness dependence of silicon porous layers and pores geometry on the parameters of etching process was established from the SEM measurements. SEM images of the porosified layers showed the homogeneity of pores on the silicon surface and, their sizes of around 8 nm, see in Fig. 9.

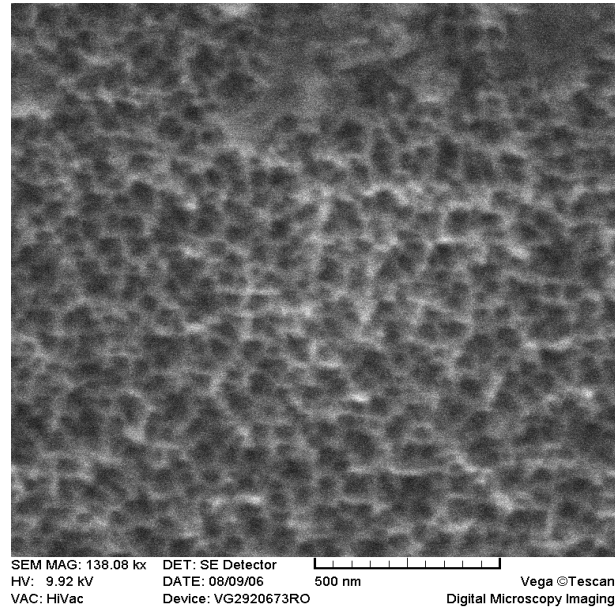


Fig. 9. SEM images of the porosified layers on the silicon surface.

5. Conclusions

An optimum technological process for texturing of the single crystalline silicon surface has been obtained.

Texturization processes application using small dimension masks leads to reflectance values smaller than 10%.

Photolithography has been used to generate patterns (holes) through the silicon dioxide layer grown at the firstly on silicon wafers. The holes have been uniformly distributed on the entire surface and the distance between the hole centers was determined to be 20 μm . Semispherical walls have been defined in holes by isotropic etching up until the walls of the adjacent walls join together.

To form pyramidal walls photolithographic process method and etching in 40% KOH solution have been used.

Texturization of an anti reflectant layer obtained by silicon oxidation leads to the lowering of the reflectivity below 5%. This method applied to solar cells leads to an

important increase of light trapping in the structure, so that conversion efficiency over 20% can be obtained.

A low-cost electrochemical etching was used to form the porous silicon layers for applications in the sensors field and in the photovoltaic cells, in order to reduce the light power losses by surface reflection. For this purpose, porous silicon layer with pore sizes in the range of 8 nm to 2 μm , depending on the conditions of formation and the characteristics of the silicon wafer, have been obtained.

References

- [1] ROHATGI A., NARASIMHA S., KAMRA S., DOSHI P., KHATTAK C. P., EMERY K., FIELD H., *Record high 18.6% efficient solar cell on HEM multicrystalline material, Proceedings of the 25th IEEE Photovoltaic Specialist Conference*, Washington DC, pp. 741–744, May 1996.
- [2] NARAYANAN S., WENHAM S. R., GREEN M. A., *17.8-percent efficiency polycrystalline silicon solar cells*, IEEE Transactions on Electron Devices, **37**, pp. 382–384, 1990.
- [3] LAUTENSCHLAGER H., LUTZ F., SCHEFFER C., SCHUBERT U., SCHINDLER R., *MC-silicon solar cells with 417% efficiency, Proceedings of the 16th IEEE Photovoltaic Specialist Conference*, pp. 7–12, 1997.
- [4] CAMPBELL P., GREEN M. A., *Light trapping properties of pyramidally textured surfaces*, J.Appl. Phys., **62**, pp. 243–249, 1987.
- [5] MANEA E., BUDIANU E., PURICA M., CRISTEA D., CERNICA I., MULLER R., MOAGAR POLADIAN V., *Optimization of front surface texturing processes on high-efficiency silicon solar cells*, Solar Energy Materials & Solar Cells, **87**, pp. 423–431, 2005.